

## MOVEMENT PATTERN OF DEBRIS FLOW

AZ. C. KANG<sup>(\*)</sup>, K.T. LAW<sup>(\*\*)</sup>, C.F. LEE<sup>(\*\*\*)</sup> & X.Q. CHEN<sup>(\*)</sup>,<sup>(\*\*\*\*)</sup>

<sup>(\*)</sup> Dongchuan Debris Flow Observation and Research Station, Chinese Academic of Sciences

<sup>(\*\*)</sup> Department of Civil and Environmental Engineering, Carleton University, Canada and visiting the University of Hong Kong

<sup>(\*\*\*)</sup> Department of Civil Engineering, the University of Hong Kong

<sup>(\*\*\*\*)</sup> Institute of Mountain Hazards and Environment, CAS, Chengdu, China

### ABSTRACT

A kinematic model is developed to estimate the velocity and runout distance of a gravitative debris flow. The characteristics and the different stages of development of a gravitative flow are first described. The equations governing the motion during the flow are then derived based on the Newtonian translation motion with some simplified assumptions on the erosion process along the flow path. After the motion is initiated, the debris is considered to behave as a frictional material with the friction angle during motion being a function of the distance travelled measured from the initiation point. The equations derived are applied to two well-documented case records to assess their applicability. The application shows that the computed runout distances are slightly higher than the measured values. This slight error on the safe side is consistent with the simplified assumptions used in deriving the equations. The small error is acceptable for engineering designs in areas vulnerable to debris flows.

**KEY WORD:** debris flow, movement pattern, kinetic mode, case record

### INTRODUCTION

Two main types of debris flow are possible in nature: hydraulic debris flow and gravitative debris flow. A hydraulic debris flow is caused by a strong surface runoff eroding large quantity of solid materials and bringing them down a ravine to become a debris flow.

A gravitative debris flow is initiated by an increase in water content in the loose soils and rocks at high elevations, which reduces the material strength that in turn causes a landslide to occur. As the mass slides down the valley, it experiences strong disturbance that leads to softening and liquefaction of the material. The sliding down of this softened or liquefied debris along the slope is called a debris flow. While a lot of studies have been conducted on the first type of debris flow (INVERSON, 1997, TAKAHASHI 1978, WU *et alii*, 1990, among others), less emphasis has been placed on the study of the second type (IVerson *et alii*, 1997). This paper presents the development of a model for describing the movement pattern involved in the second type of debris flow. The applicability of the model is examined based on two well-documented case records of gravitative debris flow. The first one occurred in Japan while the second one in Hong Kong.

### CHARACTERISTICS OF MOVEMENT PATTERNS

The first kind of debris flow is known as the hydraulic debris. The first kind of debris flow is known as the hydraulic debris flow. QIAN (1989) shows schematically the processes of initiation to full development of a hydraulic debris flow. The sediments in the channel bed, known as the static bed, go through several stages to reach the final flowing state (QIAN, 1989). Initiation of the sediment movement begins when the heavy runoff starts to impart energy to the sediments. The sedi-

ments then go into the second stage known as bed load motion. The term “bed load” is used here in the usual sense that the sediments are supported by the dispersive force stemmed from particle collisions. Relative motion exists between these sediments and the flowing water, both in the vertical direction and along the general flow direction. To sustain such relative motion, some potential energy of the flow is dissipated. In the third stage, parts of the sediments are suspended in the flow. The suspension of these particles is maintained by the turbulence in the flowing water, thus some turbulence energy is consumed. From this point on, this type of debris flow can be subdivided into two groups. In the first group, the sediments contain clayey particles exceeding a certain limit. The flow process then goes into the fourth stage in which the fine clayey particles remain in suspension to form slurry. Under this condition, there exists no relative motion between the flowing water and the clayey particles and the flow can no longer be described by the Newtonian fluid. Instead, the Bingham model should be used. As the flow continues, the turbulence energy will decrease until the flow slows down to a laminar flow. This first group is known as a viscous debris flow. For the second group, the clay content is less than the limiting value and the flow directly becomes laminar without forming slurry. This group is called a water-stone flow.

The second kind of debris flow is known as the gravitative debris flow. A schematic representation of this kind of flow is given in Figure 1. This type of debris flow normally takes place on high slopes with loose soils and fractured rocks. During rainfalls, water infiltrates into the loose soil mass, increasing the pore

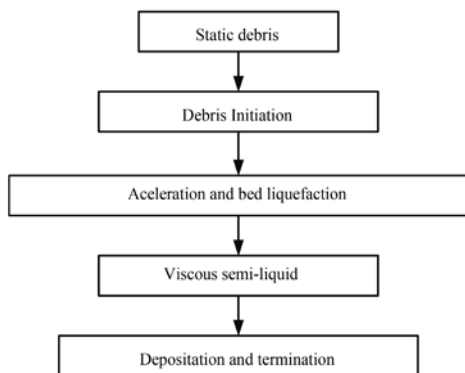


Fig. 1 - Schematic diagram showing the different stages of movement pattern in gravitative debris flow

pressure and decreasing the shear strength of the slope mass. When the decrease of strength reaches a critical value, the slope mass starts to move. A landslide or slump will follow if the situation remains critical. As the sliding mass accelerates down the slope, the bottom part of the loose mass near the sliding surface is subject to disturbance leading to softening and liquefaction. When this softened mass travels down the more gentle part of the slope, two possibilities may occur. The first is when additional water is present. The continuing motion with the addition of water will turn the debris into a semi-liquid flowing through the passing channel. The second possibility is no more additional water being present. The debris flow will then experience an increase in internal friction against the flow. In either case, the flow will eventually reach the final stage of deposition and complete termination of motion.

The first type of motion pattern above has already been well described. In this paper, a model describing the motion of the gravitative debris flow is proposed based on many years of field observations of the first author (KANG, 1989, 1991, 1997, 1999). The applicability of the model to actual case records is also illustrated.

## THE PROPOSED MODEL

For ease of discussion, the four different zones of a gravitative debris flow are shown in Figure 2: 1) source zone, 2) acceleration zone, 3) passing channel, and 4) deposition zone.

In general, loose soil and fractured rock accumulated at high concave slopes mainly come from landsliding at higher elevations of the mountain. Having subject to long-term physio-chemical weathering, the body of loose soil and rock often contains a definite amount of finer particles exhibiting some cohesive

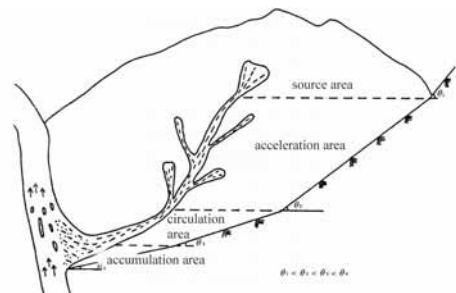


Fig. 2 - Typical flow path and cross section of a gravitative debris flow

strength,  $C$ . Under normal water content, the slope is in stable condition. During rainfall, rainwater infiltrates into the slope causing the pore water pressure to rise with the consequence that the material strength decreases. If the strength decreases to a certain point, the slope will lose its stability and start moving downwards. For some given conditions, the slide will turn into a debris flow and go through the path as shown in Figure 2. The governing equations for equilibrium or motion for each zone are discussed in the following.

**INITIATION OF DEBRIS**

There are two main approaches for considering the initiation of debris motion. The first is based on conventional soil mechanics for stability of slopes composed of unsaturated soils. Infiltration of rainwater into the soil reduces the soil suction that leads to a lowering of the apparent cohesion (FREDLUND & RAHARDJO, 1993). When the suction is completely removed, positive pore pressure will build up that reduces the effective stress and lowers the frictional resistance. When the overall strength is reduced to a critical point, a failure will occur and the slope mass will start to move. Analysis of such a process can be carried out by many existing methods. One convenient and popular method is the method of slices based on the limit equilibrium concept (e.g., BISHOP, 1955; MORGENSTERN & PRICE, 1965).

A slightly different approach is adopted here for analysing debris motion initiation in the study of debris flow. Based on large direct shear box tests on soil samples recovered from a debris flow, ZHANG (1992) demonstrated that, the strength parameters of the debris, both the cohesion ( $C$ ) and the friction angle ( $\Phi$ ),

decrease with increases in water content due to infiltrating rainwater. Based on this observation, the following is developed.

There are three stages for the increase of water content leading to the initiation of a landslide (Figure 3-a, b, and c).

The following notations are used in establishing the proposed model:

Where  $\rho_m$  and  $d_{cp}$  = density and average diameter of the solid particles, respectively;

$g$  = gravitational acceleration; and  $\Phi$  = static friction angle of the soil and rock.

Stage 1 (Figure 3-a) At this stage, the loose soil and rock in the source zone is under a stable condition without rainwater infiltration. Consideration of the stress condition leads to:

$$\tau = \rho g z \sin \theta_1 \tag{1}$$

$$\tau_c = \rho g z \cos \theta_1 \tan \phi + \rho_m g d_{cp} \tan \phi \tag{2}$$

Where  $\tau$  and  $\tau_c$  are the shear stress and the shear strength, respectively.

For stable equilibrium,  $\tau < \tau_c$ , hence:

$$\tan \theta_1 < \tan \phi + \rho_m g d_{cp} \tan \phi / \rho g z \cos \theta_1 \tag{3}$$

The second term on the right hand side of Eq.(3) is negligibly small since

$d_{cp} \ll z \cos \theta_1$  at any significant depth  $z$ . Hence Eq. (3) is reduced to:

$$\tan \theta_1 < \tan \phi_1 \tag{4}$$

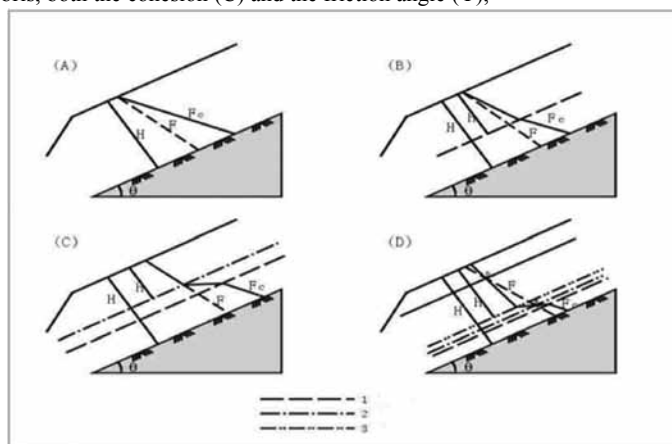


Fig. 3 - Schematic diagrams for stress distribution involved in the initiation of debris movement(1- Wetting line; 2- Water saturation line; 3- Over-saturation line)

This states that a stable condition exists if the slope angle is smaller than the static friction angle of the material.

Stage 2 (Figure 3-b)

At this stage the debris body is moistened but has not yet reached the saturation state with the infiltrating rainwater from a moderate rainfall. The moistened zone is demarcated with a moist front. The debris body is still stable as the increase in the water content has not reduced sufficiently the strength of the material to trigger a landslide. The governing condition is similar to Eq. (4).

$$\tan \theta_1 < \tan \phi_1 \tag{5}$$

Where  $\phi_1$  is the friction angle of the moist debris, which is lower than that in Stage 1.

Stage 3 (Figure 3-c)

As rainfall increases, the water content of the debris body reaches the saturation point. Hence the friction angle, now corresponding to the saturated condition, will drop further to  $\Phi_2$ . Initiation of the motion will occur if  $\tau \geq \tau_c$ . Hence

$$\tan \theta_1 < \tan \phi_1 \tag{6}$$

**ACCELERATION OF DEBRIS**

After movement is initiated, the soil and rock mass is now turned into debris that starts to accelerate down the slope. As a result of the motion, there will be a change in the physical properties in the entire body of the debris. Near the sliding surface, the debris there is fully saturated and subjected to severe mechanical disturbance. A layer of softened or liquefied soil is formed. Consequently the apparent friction angle will be reduced. As the distance of travel increases, the degree of disturbance and liquefaction increases, which in turn further reduces the apparent angle of friction. The rest of the debris will be undergoing a transition from visco-elastic solid into a visco-elastic liquid. The apparent angle of friction ( $\Phi_m$ ) at this state corresponds to the transition state. This apparent friction angle is smaller than the static friction angle.

The equations governing the motion for this state of the debris flow can be derived with the aid of Figure 4. At this state, the cohesion, C, can be considered negligible, i.e., C=0. Therefore, consideration of the Newtonian motion equation along the X-direction yields:

$$a = g \cos \theta_2 (\tan \theta_2 - \tan \phi_m) \tag{7}$$

where a = acceleration, and  $\theta_2$  = slope angle of this zone. With the initial velocity  $v_0 = 0$ , the velocity vt at any time t is given by:

$$vt = g t \cos \theta_2 (\tan \theta_2 - \tan \phi_m) \tag{8}$$

**PASSING CHANNEL**

After going through the acceleration stage, the debris mass now enters into a gentler sloping channel as a semi-solid and semi-liquid material. The motion of the debris mass depends on the presence of additional water. If additional water is available, the motion of the debris will advance to the viscous liquefied flow state. Many equations exist for computing the velocity of the flow for this condition. One well established equation is given below:

$$V_c = (gh \tan \theta_3)^{1/2} / m_c \tag{9}$$

where  $V_c$  is the velocity of the debris flow,  $\theta_3$  the slope angle of the channel, h the thickness of the debris, and  $m_c$  the resistance coefficient. The value of  $m_c$  depends on the properties of the fluid. Based on observations between 1960s and 1990s (KANG, 1999), on Jiangjia-gou Ravine, Dongchuan, Yunnan,  $m_c = 1/10 \sim 1/7$ , and from Huoshao Gully in Wudu, Gansu,  $m_c$  varies from 1/5 to 1/7.

**DEPOSITION AND TERMINATION**

The flowing mass eventually enters its last stage characterized by deposition and termination of mo-

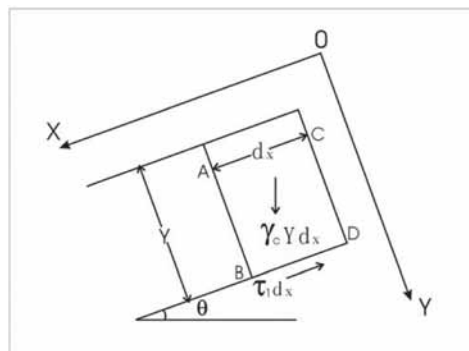


Fig. 4 - Force equilibrium of soil in X-direction

tion. Some debris mass may go through the acceleration stage and the passing channel stages before arriving at this stage while others may arrive directly from the acceleration stage. In any case, the debris mass enters this final stage without the presence of additional water. There it will encounter two kinds of resistance. Firstly the inclination of the slope ( $\theta_4$ ) usually drops from  $30^\circ$ – $25^\circ$  to  $10^\circ$ – $4^\circ$ . This severely limits the energy development of the moving debris and results in a reduction of its speed. Secondly, the surface of this zone is normally rugged and dry. The travelling viscous debris will lose some of its water into the dry ground, gradually increasing the apparent friction angle. Together, these two types of resistance will turn the visco-elastic liquid into a visco-elastic solid, eventually causing the debris to come to a halt. For this stage, the apparent friction angle  $\Phi_m$  is larger than the slope angle  $\theta_4$ . The equation of motion can be given by:

$$a = g \cos \theta_4 (\tan \theta_4 - \tan \phi_m) \tag{10}$$

Since  $\theta_4$  is less than  $\Phi_m$ ,  $a$  is a deceleration for the debris in this stage.

With the initial velocity  $= v_0$  at this stage of motion, the velocity,  $vt$ , at time  $t$  can be obtained in the same manner as in the acceleration stage. They can be expressed as:

$$vt = g t \cos \theta_4 (\tan \theta_4 - \tan \phi_m) \tag{11}$$

Since the velocity at the end of this stage is zero, the duration for this stage is given by:

$$T = - v_0 / [g \cos \theta_4 (\tan \theta_4 - \tan \phi_m)] \tag{12}$$

The distance of travel,  $S$ , in this stage can be estimated from:

$$S = v_0 T + g \cos \theta_4 (\tan \theta_4 - \tan \phi_m) T^2 / 2 \tag{13}$$

Substituting Eq.(12) into Eq.(13) yields:

$$S = v_0^2 / [2g \cos \theta_4 (\tan \theta_4 - \tan \phi_m)] \tag{14}$$

**CASE RECORDS STUDY**

The applicability of the above principles is illustrated with two well-documented case records: the Ontake debris avalanche in Japan and the Tsing Shan debris flow in Hong Kong.

*THE ONTAKE DEBRIS AVALANCHE*

The Ontake debris avalanche occurred on the southeast slope of Ontake Volcano in Japan in 1984. A saturated mass of soil and rock of  $3.6 \times 10^7$  m<sup>3</sup>, slid down the mountain at high speed along a gully and travelled over 9 km before coming to a stop at the gently sloping foothill. SASSA (1987) conducted an analysis of the debris flow using a sled model based on consideration of conservation of energy. The energy dissipated by the debris sliding over the slope is related to the apparent angle of friction ( $\Phi_m$ ) that is related to the degree of saturation of the debris and the excess pore pressure generated. The parameters for estimating  $\Phi_m$  can be obtained from high-speed ring shear tests on debris samples taken from the site. For this debris flow, the apparent angle of friction ( $\Phi_m$ ) and the slope angle of the different sections of the flow path are shown in Figure 5. By equating the change in kinetic energy and the energy dissipated by friction during the travel of the debris, SASSA (1987) estimated an average velocity of flow of 22 m/s. This velocity however cannot be verified, as there were no measurements on the actual velocity or total travel time of the debris avalanche.

The Ontake debris avalanche is reanalyzed here based on the proposed model using the same apparent friction angle as used by SASSA (1987). With reference to Figure 5, Point A is the centre of the debris mass where motion was initiated. From A to C is the acceleration zone, and from C to D is the deceleration

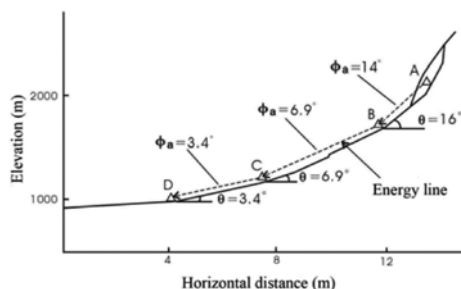


Fig. 5 - Flow path of the Ontake debris avalanche (SASSA, 1987)

zone. Point D is the motion termination point to be estimated in the proposed model

For the acceleration zone, there is a change in the slope angle breaking up the zone into two sections. The acceleration in each of the sections is therefore different. Based on Eq (7), the acceleration of the upper section with a slope angle ( $\theta$ ) of  $16^\circ$  is estimated to be  $0.346 \text{ m/s}^2$ . The corresponding velocity at B is found to be  $23.52 \text{ m/s}$  and the duration for the debris to move through this section is calculated to be  $68 \text{ s}$ . For section BC, the acceleration is approximately zero as the slope angle is equal to the apparent friction angle. Using a similar approach, the velocity at C is  $23.52 \text{ m/s}$  and the duration through this section is  $287 \text{ s}$ . For the deceleration zone C to D, application of Eq. (10) and Eq. (12) leads to a deceleration of  $0.137 \text{ m/s}^2$ , duration of  $172 \text{ s}$  and the average velocity of  $11.74 \text{ m/s}$ .

Based on this model, the total time for the complete travel of the debris avalanche is estimated to be  $527 \text{ s}$  with an average speed of  $18.26 \text{ m/s}$ . Hence the estimated distance of travel is about  $9.5 \text{ km}$ . This distance is remarkably close to the observed value of  $9 \text{ km}$ , giving support to the validity of the model.

### THE TSING SHAN DEBRIS FLOW

The Tsing Shan debris flow took place in the new Territories, Hong Kong in September 1990. This debris flow is the largest recorded landslide in natural terrain in the recent history of Hong Kong. Approximately  $19,000 \text{ m}^3$  of soil and rock was involved in the landslide and the debris trail reached about  $1035 \text{ m}$ . As the landslide occurred in an undeveloped area, there was no injury and damage to facilities was negligible. Details of the debris flow were described by KING (1996).

The debris flow occurred during a heavy rainstorm on a thick deposit of granite colluvium overlying completely decomposed granite. The rainfall triggered a small landslide, which in turn initiated a larger parent landslide with a volume exceeding  $2000 \text{ m}^3$  on the steep upper slopes of Tsing Shan. It was this parent landslide that instigated the debris flow. The parent sliding mass started to accelerate downslope, eroding and sweeping away the bouldery colluvium for about  $300 \text{ m}$ . It then reached the more gentle part of the slope where the process of deposition began. The larger pieces of boulders were first deposited forming a bouldery lateral ridge. Here, a concrete water intake was badly damaged by the boudery debris. The

finer part of the debris, mainly of gravel and sand not exceeding  $20 \text{ mm}$  in diameter, continued to move on in the form of a slurry for another  $500 \text{ m}$ . The slurry moved slowly and non-erosively around obstacles. Its potential hazard to existing structures was low.

The observed movement pattern of the Tsing Shan debris flow closely conforms to a classic example of the gravitative debris flow in which a sliding mass transforms into a debris flow. The three zones can be clearly identified: the source zone, the acceleration zone and the deposition zone. In this case record, the acceleration zone and the passing channel were merged into one. The method of analysis proposed herein is again applied to this case to test its validity.

The parameters and results used in the method are summarized in Table 1. For each zone, the material type and the geometric parameters have been obtained by KING (1996) and listed in the upper part of Table 1. Based on this information, the model is applied.

The first parameter to be obtained is the static friction angle,  $\Phi$ , for the debris material. This material is largely composed of granite colluvium. Based on its particle size (ignoring the boulders), the colluvium is a gravelly, silty sand. Although there are no triaxial test results on this material, a lot of test results on materials similar to this are available in Hong Kong. Based on such information (e.g., Geoguide I 1993), a value of  $38^\circ$  is chosen for  $\Phi$  for this material.

The next parameter to be obtained is the apparent friction angle  $\Phi_m$  for the material. To be rigorous, highly specialized experimental equipment, such as the high speed ring shear device, is required for its determination. At present no such data exist for this case record. However one can use the relationship established for the Ontake debris avalanche as a first approximation. This relationship can be written as:

$$\tan \phi_m = Km \tan \phi$$

where  $Km$  is a factor dependent on the distance of travel of the debris and can be derived from Figure 5. The  $\Phi_m$  values thus computed are listed in Table 1

Based on calculations similar to those in the previous case, the velocities of the debris mass at different points and stages of the flow path are summarized in Table 1. The estimated stopping point of the debris flow or the leading edge of the debris is marked by point D on Figure 6, while the corresponding meas-

mmZones Characteristics	Source zone		Acceleration zone	Deposition zone	
	Trigger landslide	Parent landslide		Passing channel	Debris containing large number of boulders
<sup>1</sup> Material	Up to 2 m loose angular granite spur colluvium, estimated boulder content 62% to 83%, matrix of low plasticity, clayey very silty very gravelly sand	Up to 6 m of loose angular spur colluvium, estimated boulder content 62% to 85%, matrix of low plasticity clayey very silty very gravelly sand with 17 - 28% fines	Up to 3 m of valley colluvium, estimated boulder content 69% to 87%, matrix of low plasticity clayey silty, gravel and sand with 15 - 20% fines.	Debris vegetation, boulders, cobbles, in a silty sandy gravel matrix with local variation of proportion of clast to matrix, estimated boulder content > 57%, matrix of low plasticity clayey silty very gravelly sand, 17 - 26% fines	Debris, composed mainly of matrix of gravel, sand, silt and clay deposited from liquefied debris moving beyond the first part of deposition
<sup>1</sup> Mobility moisture	21 - 36%	28 - 40%	25 - 37%	28 - 30%	28 - 30%
<sup>1</sup> Slope angle (Length)	> 40° (38 m)	28° (61 m)	A - B 35° (50 m) B - C 28° (310 m)	C - D 11° (180 m)	D - E 6°, 2° (350 m)
<sup>1</sup> Movement type	Slump	Slump	Acceleration	Deceleration to stop	Flow and deposition
<sup>2</sup> Static friction angle	38°				
<sup>3</sup> Apparent friction Angle	24°		23°	20°	
<sup>1</sup> Debris velocity			A - B 0 - 10 m/s B - C 10 - 27.1 m/s	27.1 - 0 m/s	8.1 - 4.6 m/s
<sup>2</sup> Average velocity			12.4 m/s	13.5 m/s	6.4 m/s
<sup>1</sup> Rainfall	8 mm/5 min		53 mm/1 hour	91.5 mm/2 hours	151 mm total

<sup>1</sup> adapted from King 1996; <sup>2</sup> assumed; <sup>3</sup> calculated from the present model

Tab. 1 - Movement characteristics at different stages of the Tsing Shan debris flow

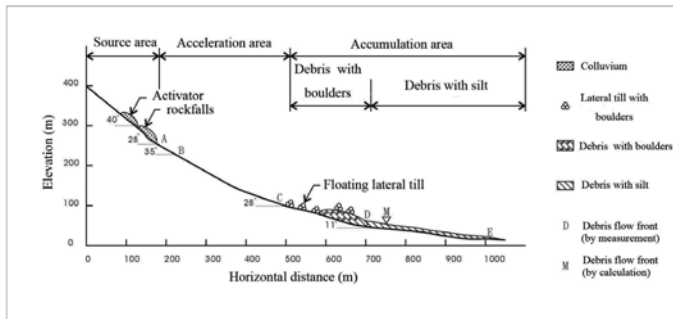


Fig. 6 - Flow path of the Tsing Shan debris flow

ured point is marked as M in the same figure. The distances from A to D and to M are 505 m and 555 m, respectively. Comparing these two points, it is obvious that the estimated stopping point is slightly ahead of the actual one. The agreement between the estimated and the measurement is quite acceptable recognizing the approximation used in establishing  $\Phi_m$ .

**DISCUSSION**

The runout distance of a debris flow is equal to the distance between the initiation point to the final point of stoppage. The application of the proposed model has shown that the proposed model yields a runout distance slightly larger than the measured values. There is one major reason for this discrepancy. The model assumes that once initiated the debris continues its journey down the slope with no addition of materials. In reality in the acceleration zone, erosion of in-situ materials is quite likely. This will add mass to the debris and will consume part of the original kinetic energy in the flowing mass. Hence the actual runout distance will be shorter than that is obtained from the model.

The discrepancy between the measured and the actual runout distance based on the proposed model is small. The discrepancies for the Ontake debris avalanche and for the Tsing Shan debris flow are 5% and 9%, respectively. This discrepancy errs on the safe side. Recognizing the many uncertain factors involved in a debris flow, this discrepancy is acceptable for design consideration.

A reliable method for estimating the runout distance has great value in construction and development in areas vulnerable to debris flow. The present method erring on the safe side by about 10% provides a useful tool for locating facilities in areas vulnerable to debris flow occurrence. Hence this method will help reduce hazards and risks for developments in debris flow zones.

**SUMMARY AND CONCLUSIONS**

Based on past observations, a general movement pattern is described for the gravitative debris flow in which a landslip or slump is transformed into a debris flow. A simple kinematic model is proposed for characterizing the different stages of a gravitative

debris flow. From the model, the runout distance of the debris flow can be determined. The model has been applied to two well-documented records. The first one is the Ontake Volcano debris flow in Japan and the other is the Tsing Shan debris flow in Hong Kong. Comparison has been made between the estimated and the observed runout distances for these two debris flows. The estimated values are within 10% higher than the observed values. The reason for the estimated value being higher is due to the simplified assumption of ignoring the added mass to the debris due to erosion along the path of the debris flow. Recognizing the highly complex nature of debris flows, one may conclude that the proposed model gives excellent estimates of the actual runout distances of debris flows. Furthermore the simplified assumption leads not only ease of calculation, but it

also gives a result slightly on the safe side. Hence this approach has a good potential for design applications in areas vulnerable to debris flows.

## ACKNOWLEDGEMENTS

The research is supported by National Basic Research Program of China (Grant No. 2011CB409903), and the Hong Kong Jockey Club Charities Trust. The authors express deep appreciation to Mr. Y.C. Chan and Dr. D. Lo, both of the Geotechnical Engineering Office, Hong Kong SAR Government, for their conscientious efforts in taking the authors for a tour of the Tsing Shan debris flow site and for providing valuable information on the failure. This paper is published with the financial support of the Jockey Club Charities Trust and the Research Grant Council of Hong Kong.

## REFERENCES

- BISHOP A.W. (1955) - *The use of the slip circle in the stability of slopes*. Geotechnique, **5**: 7-17.
- FREDLUND D.G. & RAHARDJO H. (1993) - *Soil mechanics for unsaturated soils*. Wiley, New York.
- GEOGUIDE 1 (1993) - *Guide to Retaining Wall Design*. Geotechnical Engineering Office, Hong Kong SAR Government.
- IVERSON R.M., (1997) - *The physics of debris flow*. Reviews of Geophysics, **35**(3): 245-296.
- IVERSON R.M., REID M.E. & LAHUSEN R.G. (1997) - *Debris-flow mobilization from landslides*. Annu. Rev. Earth Planet. Sc., **25**: 85-138.
- KANG Z.C. (1987) - *Mechanic analysis on the occurrence of debris flow*. Research of Mountain, **5**(4): 225-229 (in Chinese).
- KANG Z.C. (1991) - *Mechanic analysis on the acceleration of viscous debris flow*. Research of Mountain, **9**(3): 193-196, (in Chinese).
- KANG Z.C. (1997) - *Kinetic analysis on the deceleration and deposition process of viscous debris flow*. Proceedings of the First International Conference on Debris Flow, San Francisco, USA: 153-157.
- KANG Z.C. (1999) - *Generation, Movement and Sedimentation of Viscous Debris Flow*. Joint Research Report of the Special Project No.951105 Sponsored by the Chinese Academy of sciences and Ministry of Water Conservancy and the Group C3 of Special Project associated with IDNDR Sponsored by Ministry of Education, Science, Sports and Culture, Japan: 30-41.
- KING J.P. (1996) - *The Tsing Shan debris flow*. Geotechnical Engineering Office, Hong Kong SAR Government, SPR 6/96, 3 Vol.
- MORGENSTERN N. R. & PRICE V.E. (1965) - *The analysis of the stability of general slip surfaces*. Geotechnique, **23**: 121-131.
- QIAN N. (1989) - *Motion of concentrated water*. Tsinghua University Press: 7-9.
- SASSA K. (1987) - *The Ontake debris avalanche and its interpretation*. Landslide News, **1**: 6-8.
- SCHAMBER D.R., & MACARTHUR R.C. (1985) - *One-dimensional model for mud flows*. In: Hydraulics and Hydrology in the Small Computer Age, Vol. 1, ASCE, 1334-1339.
- TAKAHASHI, T. (1978) - *Mechanical characteristics of debris flow*. Journal of Hydraulic Div., Proc. ASCE, **103**(3): 381-396.
- WU J.S., KANG Z.C., TIAN L.Q. & ZHANG S.C. (1990) - *Observational research on debris flow in the Jiangjia Ravine of Yunnan Province*. Chinese Sciences Press: 53-98, (in Chinese).
- ZHANG J (1992) - *The mechanical characteristics of debris from debris flows and their application in engineering designs and preventive measures*. Dongchuan Debris Flow Observation and Research Station, Chinese Academy of Sciences (in Chinese)